Available online at www.sciencedirect.com
ScienceDirect
Journal of Organometallic Chemistry 693 (2008) 1321–1334
Journal of Organometallic Chemistry
www.elsevier.com/locate/jorganchem

Synthesis, crystal structure and non-linear optical properties of boronates derivatives of salicylideniminophenols

Blanca M. Muñoz [a], Rosa Santillan [a,*], Mario Rodríguez [a], José Manuel Méndez [b], Margarita Romero [b], Norberto Farfán [b], Pascal G. Lacroix [c], Keitaro Nakatani [d], Gabriel Ramos-Ortíz [e], José Luis Maldonado [e]

[a] Departamento de Química, Centro de Investigación y de Estudios Avanzados del IPN, 07000, Apdo, Postal 14-740, México D.F., Mexico
[b] Facultad de Química, Departamento de Química Orgánica, Universidad Nacional Autónoma de México, México D.F. 04510, Mexico
[c] Laboratoire de Chimie de Coordination du CNRS, 205 Route de Narbonne, 31077 Toulouse, France
[d] Laboratoire de Photophysique et Photochimie Supramoléculaires et Macromoléculaires (UMR 8531 du CNRS), Ecole Normale Supérieure de Cachan, Avenue du Président Wilson, 94235 Cachan, France
[e] Centro de Investigaciones en Óptica, A.P. 1-948, 37000 León, Gto., Mexico

Received 10 August 2007; received in revised form 18 January 2008; accepted 18 January 2008
Available online 26 January 2008

Abstract

The condensation in one step of a series of salicylaldehydes and 2-amino-5-nitrophenol with 1-naphthylboronic acid, 2-naphthylboronic acid, and *o*-tolylboronic acid to give the corresponding boronates **1a**–**3a**, **1b**–**3b** and **1c**–**3d**, is reported. The X-ray crystal structures of **1a**, **2b** and **3b** allowed determining the α- and β-angle between the stilbene skeleton and the aryl or naphthylboronic fragments; these values are indicative of different conformations for the aryl moieties around the (B–C) boron–carbon bond which could potentially modulate the electronic properties on the boron stilbene compounds. All compounds were characterized by ^{1}H, ^{11}B and ^{13}C NMR spectroscopy, UV, IR and mass spectrometry. Second- and third-order non-linear optical characterizations were also performed by EFISH and THG Maker Fringe techniques, respectively. Compounds **3a**–**3d** containing an $-N(Et)_2$ donor group gave the best NLO response in second- and third-order.

Keywords: Boronates; NLO; ^{11}B NMR; X-ray

1. Introduction

The great versatility of boron chemistry has led to a number of applications of these compounds in medicinal [1], supramolecular [2] and materials chemistry [3]. In particular, stabilization through the formation of complexes containing dative N → B bond has been studied intensively [4], some examples include the condensation of boronic acids with ethanolamine [5] or amino acids [6].

The organic boron compounds are interesting species with optoelectronic properties, in particular for non-linear optics (NLO), where the three-coordinate species have been more widely studied due to the fact that the vacant p orbital is a strong π-electron acceptor which can lead to significant delocalization with an adjacent organic π-system [7] (Fig. 1).

Other boron species with NLO properties are the zwitterionic systems (Fig. 2), where the boron atom has a negative charge and the nitrogen is an ammonium salt. These systems show high ground-state dipole moments and are expected to have a small dipole moment in the first excited singlet state [8].

Complexes containing the N → B coordinated bond which are derived from pyridine and Lewis acids such as BF_3 or $B(C_6F_5)_3$ present excellent NLO properties due to the fact that formation of the pyridyl-boron complex leads

* Corresponding author. Tel.: +52 55 50 61 37 25; fax: +52 55 50 61 33 89.
E-mail address: rsantill@cinvestav.mx (R. Santillan).

0022-328X/$ - see front matter © 2008 Elsevier B.V. All rights reserved.
doi:10.1016/j.jorganchem.2008.01.032

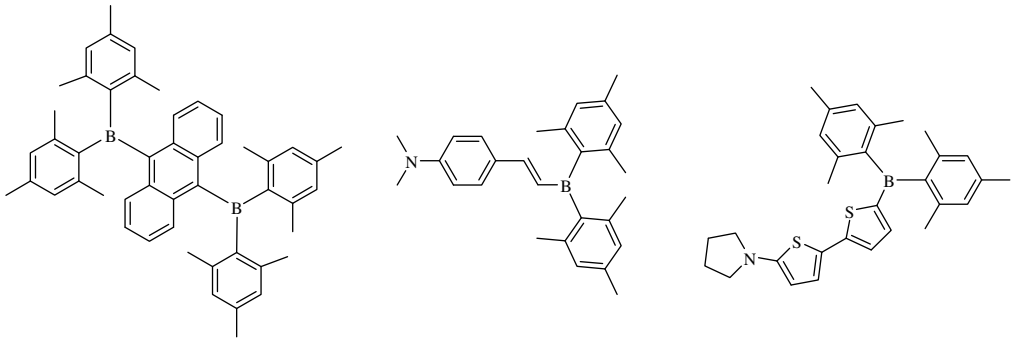

Fig. 1. Dimesityl boron compounds with attractive NLO properties.

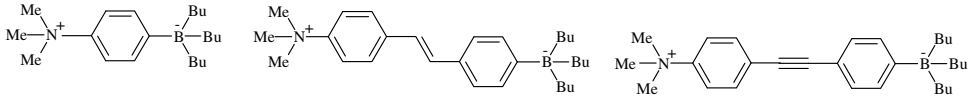

Fig. 2. Borate Zwitterionic salts with high dipole moments.

to enhancement of the withdrawing effect and consequently of second-order NLO properties [9] (Fig. 3).

It has been reported that compounds containing boron and other elements such as bismuth exhibit promising non-linear optical properties, for example, BiB_3O_6 (BIBO) shows large second-harmonic generation (SHG) coefficient compared to other known NLO borates such as BBO and LiB_3O_5. In addition, bismuth borates crystallize in non-centrosymmetric space group, this is an important prerequisite in the search toward solid state NLO properties [10].

Other compounds commonly employed in non-linear optics are donor–acceptor substituted π-electron systems, such as subphthalocyanines which exhibit good NLO properties. These compounds are planar and with excellent physicochemical properties, including high aromaticity, very good thermal and chemical stability (Fig. 4) [11].

We recently reported the synthesis and non-linear optical properties of "push–pull" boron chromophores containing the well-known stilbene backbone with an arylboron (ArB) group (Fig. 5) [12]. The results suggest that modulation could be achieved by rotation of the phenyl around the boron–carbon bond. One of these boron chromophores has been used for NLO dynamic holographic imaging in photorefractive polymers [13].

Also, a series of boron complexes derived from hydroxychalcones with borontrifluoride and diphenylborinic acid has been reported [14] (Fig. 6). These boron complexes exhibit a delocalized "push–pull" system. Unfortunately they decomposed in solution, and in the solid state they

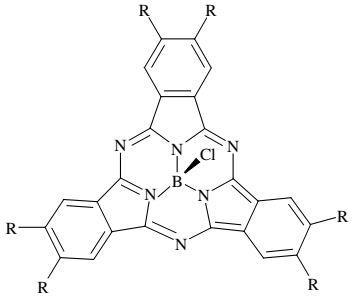

R = *p*-Tolylthio, *p*-tolylsulfonyl, SC_8H_{17}, $SO_2C_8H_{17}$

Fig. 4. Boron complex of subphthalocyanines with NLO properties.

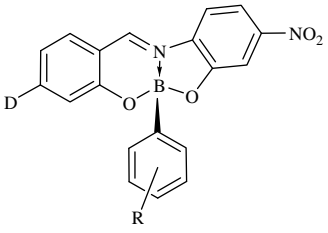

D = OMe, $N(Et)_2$

R = H, Cl, OMe, Br, F, NO_2, CHO

Fig. 5. Boron compounds derived from Schiff Bases with NLO properties.

crystallized in centrosymmetric space groups, therefore the NLO properties are canceled.

In continuation of our research, we designed a series of push–pull boronates that contain an aryl- or naphtyl

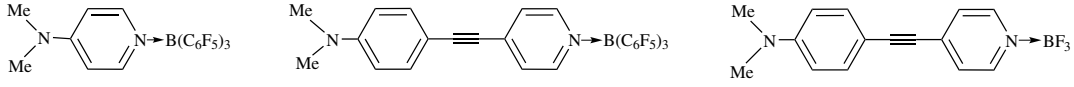

Fig. 3. Pyridine-boron complex with NLO properties.

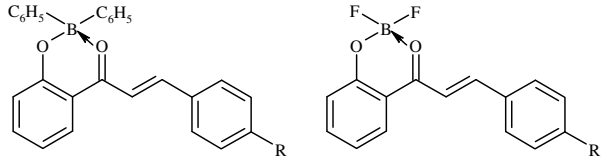

Fig. 6. "Push–pull" boron complexes derived from hydroxychalcones.

boronic acid fragment in order to investigate the preferential conformation around the B–CPh bond and their potential application to modulate the NLO response using different substituents. The complexes are stable and were obtained in high yields through an easy one-step synthesis.

2. Results and discussion

2.1. Synthetic aspects

The tridentade ligands **1**–**3** were prepared by condensation of the appropriate salicylaldehyde with 2-amino-5-nitrophenol [15,17]. The boron compounds **1a**–**3a**, **1b**–**3b** and **1c**–**3c** were obtained in one step by condensation of the salicylaldehyde with 2-amino-5-nitrophenol and the corresponding boronic acid. The reactions were carried out under reflux of acetonitrile and a catalytic amount of acetic acid from 2 to 8 h to give the corresponding boronates in yields between 81% and 90% except for compounds **2c** (65%) and **3b** (54%) (Scheme 1).

To modulate the NLO response through different conformations around the B–C bond, a series of boron complexes containing different boronic acids were prepared. In addition, **3d** containing an aldehyde group in the *ortho* position was synthesized with the aim to fix the orientation of the boronic acid fragment through an intramolecular hydrogen contact with the phenolic oxygen. This molecule was obtained in two steps, since the one step procedure leads to a mixture of compounds (Scheme 2).

2.2. Spectroscopic data

All compounds were characterized by ^{1}H, ^{11}B and ^{13}C NMR; selected data is summarized in Table 1. The singlets between 8.15 and 8.77 ppm in the ^{1}H NMR spectra of compounds **1a**–**3a**, **1b**–**3b**, **1c**–**3c** and **3d**, correspond to the imine proton and confirm the formation of the Schiff base. The signals for H-22 are shifted to high frequencies (8.82, 8.81 and 8.84 ppm) for compounds **1a**–**3a** which have a 1-naphthyl substituent, due to the existence of an intramolecular interaction with the O-2 (phenolic moiety), as confirmed by the solid state analysis of compound **1a** (H-22···O2 2.513(2) Å).

The ^{1}H NMR signals for the aryl and naphthyl rings were assigned based on their COSY spectra which allow correlation between the protons in the ring containing the electron-withdrawing group and those of the ring with the electron-donating group. The COSY spectra were necessary because the multiplicity and chemical shifts of some signals are very similar.

In the ^{13}C NMR spectra of boron derivatives **1a**–**3a**, **1b**–**3b**, **1c**–**3c** and **3d**, the signals for C2 are shifted to low frequencies (157.1–158.9 ppm), with respect to the ligands

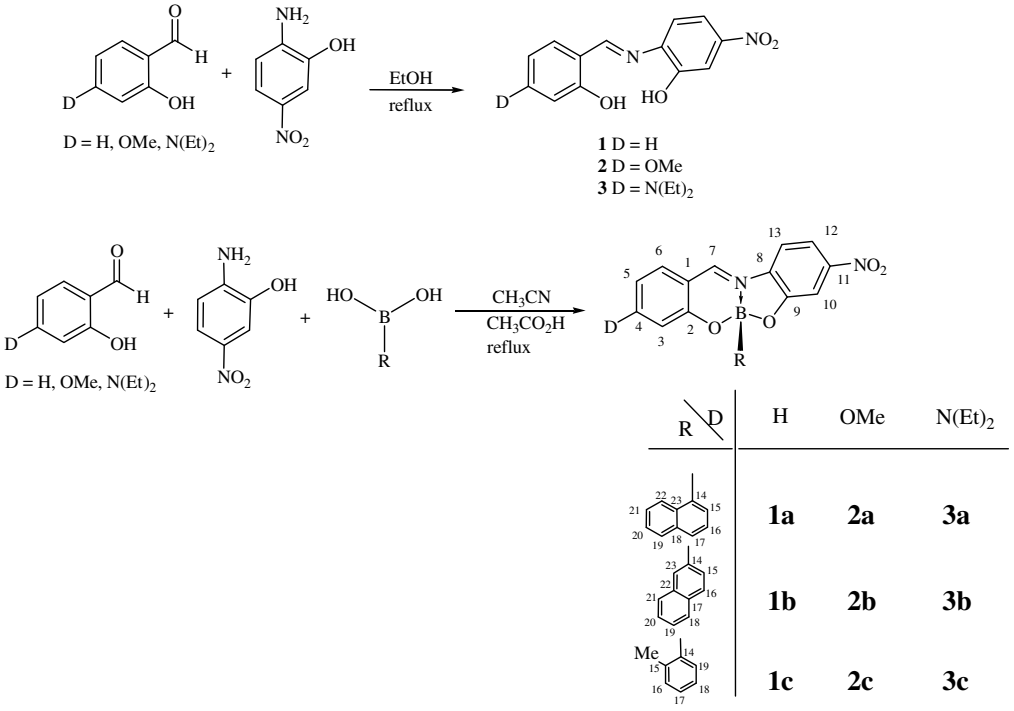

Scheme 1. Synthesis of ligands **1**–**3** and boronates **1a**–**3a, 1b**–**3b** and **1c**–**3c**.

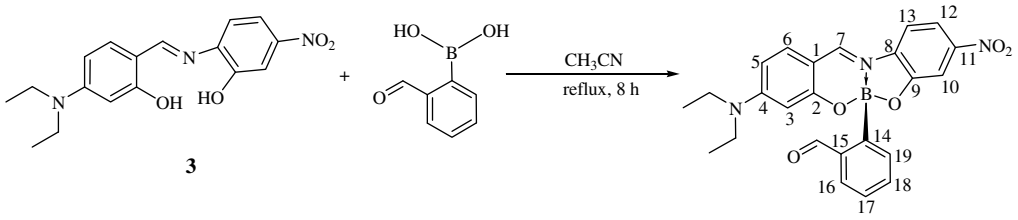

Scheme 2. Synthesis of boronate **3d**.

Table 1
Selected ^{1}H, ^{11}B, ^{13}C NMR (ppm) and IR (cm^{-1}) data for compounds **1**–**3**, **1a**–**1c**, **2a**–**2c** and **3a**–**3d**

Compound	^{1}H NMR (ppm) (H-7)	^{13}C NMR (ppm)				^{11}B NMR (ppm)	IR (C=N) (cm^{-1})
		C-2	C-4	C-7	C-9		
1	9.01	161.2	134.5	165.5	151.7		1624
2	8.97	161.6	165.3	161.8	146.0		1620
3	8.79	167.2	159.2	152.5	144.4		1619
1a	8.77	158.3	139.7	152.7	157.7	9.8	1629
1b	8.55	158.9	140.4	152.9	158.7	8.6	1626
1c	8.73	158.5	139.9	148.6	157.8	9.3	1617
2a	8.61	161.1	169.8	151.3	157.6	9.8	1608
2b	8.63	161.0	169.6	153.0	157.5	8.0	1606
2c	8.55	161.1	169.9	151.2	157.7	9.2	1613
3a	8.34	160.5	157.1	148.4	156.9	9.5	1606
3b	8.15	157.5	161.1	148.6	157.1	8.3	1606
3c	8.33	157.1	160.6	148.5	157.0	9.1	1607
3d	8.39	157.2	160.0	148.7	156.4	8.8	1607

(161.2–167.2 ppm) owing to the coordination to boron. In general the signal for the imine carbon (C-7) shows a marked shielding effect (148.4–153.0 ppm) compared to the ligands (152.5–165.5 ppm) due to increased delocalization of the NEt_2 substituent at the *para* position after formation of the N → B bond.

The ^{11}B NMR spectra for the 10 new compounds show one broad signal between 8.0 and 9.8 ppm indicative of tetracoordinated boron atoms [16]. In general, the C=N stretching vibration bands for compounds **2a**–**2c** and **3a**–**3d** were shifted to lower wavenumbers in comparison with the ligands, evidencing a decrease in strength as the new N → B dative bond is formed [17].

Comparison of the absorption data for compounds **1a**, **2b**, **3b** with the corresponding ligands evidences a red shift. Moreover, this shift is observed both experimentally and theoretically, as the push–pull character increases from **1a** to **3b**. It is surprising that the modest shift (5 nm) induced by the methoxy substituent when **1a** and **2b** are compared can lead to unexpected NLO effects (*vide infra*) (see Table 2).

2.3. Molecular structure

For compounds **1a**, **2b** and **3c**, it was possible to obtain crystals suitable or X-ray diffraction by slow evaporation of a concentrated mixture of $CHCl_3$ and hexane. The details of the crystal data and summary of the collection parameters for compounds **1a**, **2b** and **3b** are given in Table 3, selected bond distances and bond angles are compared in Table 4 and the molecular structures are shown in Fig. 7. Even if the boron compounds have similar structures, they crystallize in different space groups. Compound **1a** belongs to the orthorhombic space group *Icab*, **2b** to the triclinic space group $P\bar{1}$ and **3b** to the monoclinic $C2/c$. Boron

Table 2
Experimental absorption maxima (λ_{max} in nm) and extinction coefficients (ε in $dm^3\ mol^{-1}\ cm^{-1}$) are compared to ZINDO calculated data for **1a**, **2b**, and **3b**

Compounds	Experimental data		Computed data	
	λ_{max}	ε	λ_{max}	f
1	375	76489		
2	376	71215		
3	436	89920		
1a	456	11700	402	0.44
2b	461	22100	412	0.35
3b	511	31104	434	0.74

Table 3
Crystal data for **1a**, **2b** and **3b**

	1a	**2b**	**3b**
Chemical formula	$C_{23}H_{15}BN_2O_4$	$C_{24}H_{17}BN_2O_5$	$C_{27}H_{24}BN_3O_4$
Formula weight	394.18	424.21	465.30
Crystal system	Orthorhombic	Triclinic	Monoclinic
Space group	*Icab*	$P\bar{1}$	$C2/c$
a (Å)	17.3609(4)	9.9720(2)	24.5993(49)
b (Å)	17.9031(4)	11.7388(3)	19.9916(40)
c (Å)	24.5085(6)	19.7668(6)	11.6876(23)
α (°)	90.0	73.9830(10)	90
β, (°)	90.0	88.8340(10)	109.973(30)
γ (°)	90.0	66.7130(10)	90
V ($Å^3$)	7617.6(3)	2032.54(9)	5402.02(627)
Z	16	4	8
Temp (K)	293(3)	293(2)	293(2)
Reflection collected	7979	13909	18060
Reflection unique	4285	8156	5405
Reflection observed (4σ)	2501	4909	2346
Number of variables	332	714	401
Final R (4σ)	0.0462	0.0564	0.0715
Final wR_2	0.1027	0.1329	0.175
Goodness-of-fit	1.007	1.019	0.965

Table 4
Selected bond lengths (Å) and angles (°) for **1a**, **2b** and **3b**

Lengths (Å)				Angles (°)			
	1a	**2b**	**3b**		**1a**	**2b**	**3b**
O(1)–B(1)	1.498(2)	1.497(3)	1.464(4)	O(1)–B(1)–O(2)	111.16(13)	112.4(2)	111.3(2)
O(2)–B(1)	1.458(2)	1.456(3)	1.509(4)	O(2)–B(1)–C(14)	112.41(14)	113.5(2)	110.3(3)
B(1)–N(1)	1.585(2)	1.594(3)	1.572(4)	O(1)–B(1)–C(14)	113.12(14)	111.5(2)	112.9(3)
B(1)–C(14)	1.607(2)	1.606(4)	1.605(5)	O(1)–B(1)–N(1)	100.13(13)	99.55(18)	108.0 (3)
C(1)–C(7)	1.427(3)	1.420(4)	1.388(4)	O(2)–B(1)–N(1)	106.61(13)	107.51(19)	99.5(2)
C(7)–N(1)	1.296(2)	1.296(3)	1.324(4)	N(1)–B(1)–C(14)	112.60(14)	111.5(2)	114.0(3)
N(1)–C(8)	1.411(2)	1.416(3)	1.396(4)				

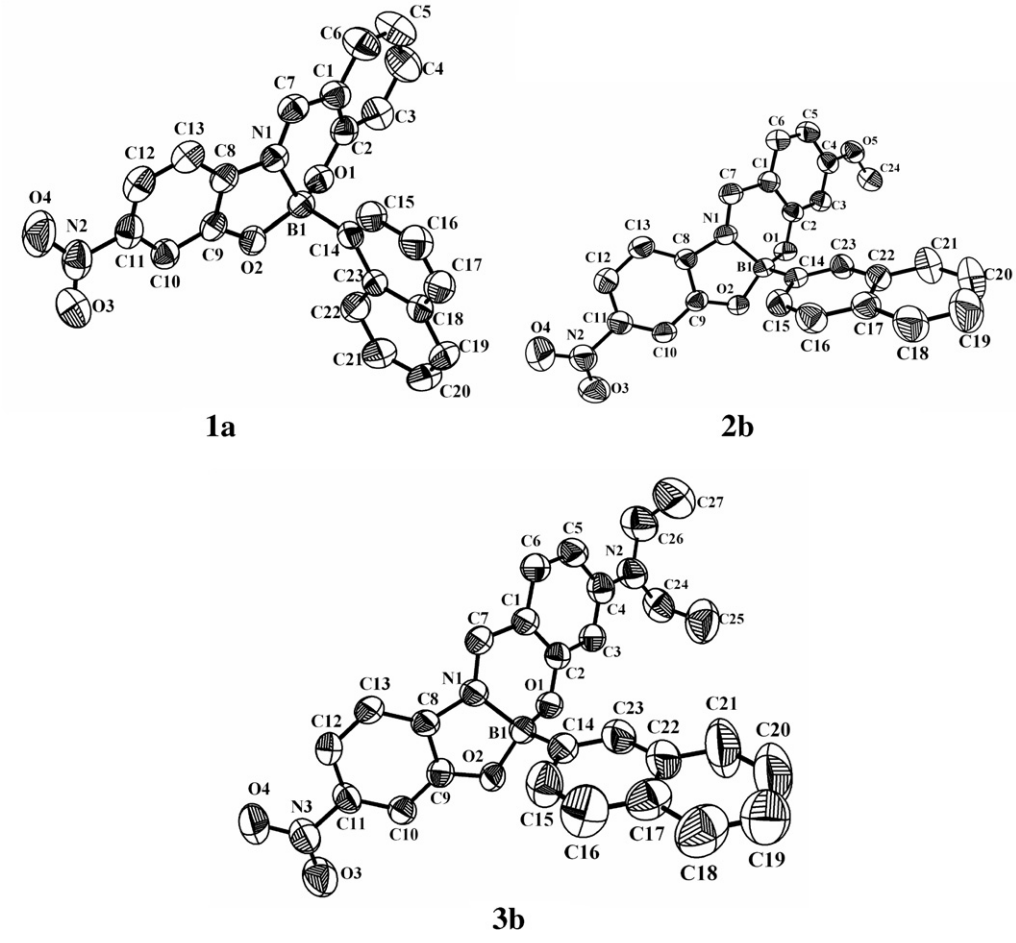

Fig. 7. X-ray molecular structure of compounds **1a**, **2b** and **3b**.

compounds **1a** and **3b** contain one crystallographically independent molecule while **2b** has two independent molecules that show the same structure in the asymmetric unit. The bond distance observed in the dative N → B and covalent B–O bonds, as well as the angle values are very similar in the three derivatives. Compounds **1a**, **2b** and **3b** contain four-coordinated boron atoms with tetrahedral character values of 74% (**1a**), 75% (**2b**) and 76% (**3b**) [18], therefore the delocalization of the π system is not optimal. The values for the intramolecular N → B dative bonds are 1.585 (2) Å, 1.594 (3) Å and 1.572 (5) Å for **1a**, **2b** and **3b** respectively, which are shorter than dimeric, oligo- and oxo-bridged boronates [19] but similar to the values reported in other monomeric boronates [12].

In turn, the N(1)–C(7) [1.324 (5) Å] bond length for compound **3b** is significantly longer than that of **2b** [N(1)–C(7) 1.296 (3)] Å and **1a** [N(1)–C(7) 1.296 (2)] showing the influence of the electron donor groups. These compounds are bent along the N → B bonds as expected in this family of boronates, as a result of the tetrahedral geometry around the boron atom. The angles around this boron atom are close to tetrahedral and the shorter value (around 100°) corresponds to O(1)–B–N. The slight folding in the molecular skeleton decreases the π-conjugation pathway

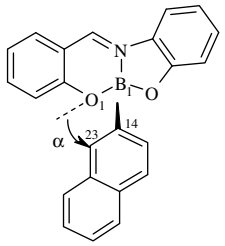

Scheme 3. The α-angle in boronate compounds.

and the NLO response. An important difference between the three molecular structures is observed in the relative orientation of the 1- and 2-naphthyl moiety with respect to the stilbene backbone which could lead to variations in NLO properties. Using the definition of the rotation α-angle (O1–B1–C14–C23) shown in Scheme 3, the crystal structure provides values of −67.3°, +4.3° and +1.1° for **1a**, **2b** and **3b**, respectively. Interestingly, the α-angle in **1a** depends on the nature of the substituent bonded to the *ortho* carbons in the aryl moiety. The results show that the 1-naphthyl group modifies the angle much more than the 2-naphtyl. The 1-naphtyl (Fig. 8) shows two intramolecular hydrogen bonds (H22···O2 2.513(2) Å, H15···N1 2.536 (18) Å) which are less than the sum of the van der Waals radii (H···O 2.77 Å, H···N 2.75 Å) [20]. In the solid state, the naphthyl fragment linked to the boron atom is perpendicular to the organic ligand, as reported for the (dppy)B-2-naphthyl complex [21].

The molecular packing diagrams of **1a**, **2b** and **3b** are depicted in Fig. 8. Compound **1a** shows a π–π stacking intermolecular interaction between the aromatic rings with a contact distance of 3.218 (3) Å that is shorter than the value reported for (dppy)B-2-naphthyl (3.40 Å)[21]. Also, the π–π stacking interaction between naphthyl groups shows a value of 3.29 (3) Å. The crystal packing of **2b** shows a chain arrangement; within each chain and there is π–π stacking interaction with ligand/ligand rings contact distances of 3.275(4) Å that is almost the same as that of (dppy)B–F (3.28 Å) [22] but shorter than the (dppy)-B–C_6H_4-2(OEt) (3.342 Å) probably due to steric effects [21].

In **3b**, two molecules are linked by two hydrogen bonds (CH···O–N 2.527(5) Å, CH···O–N 2.556 (6) Å) of the

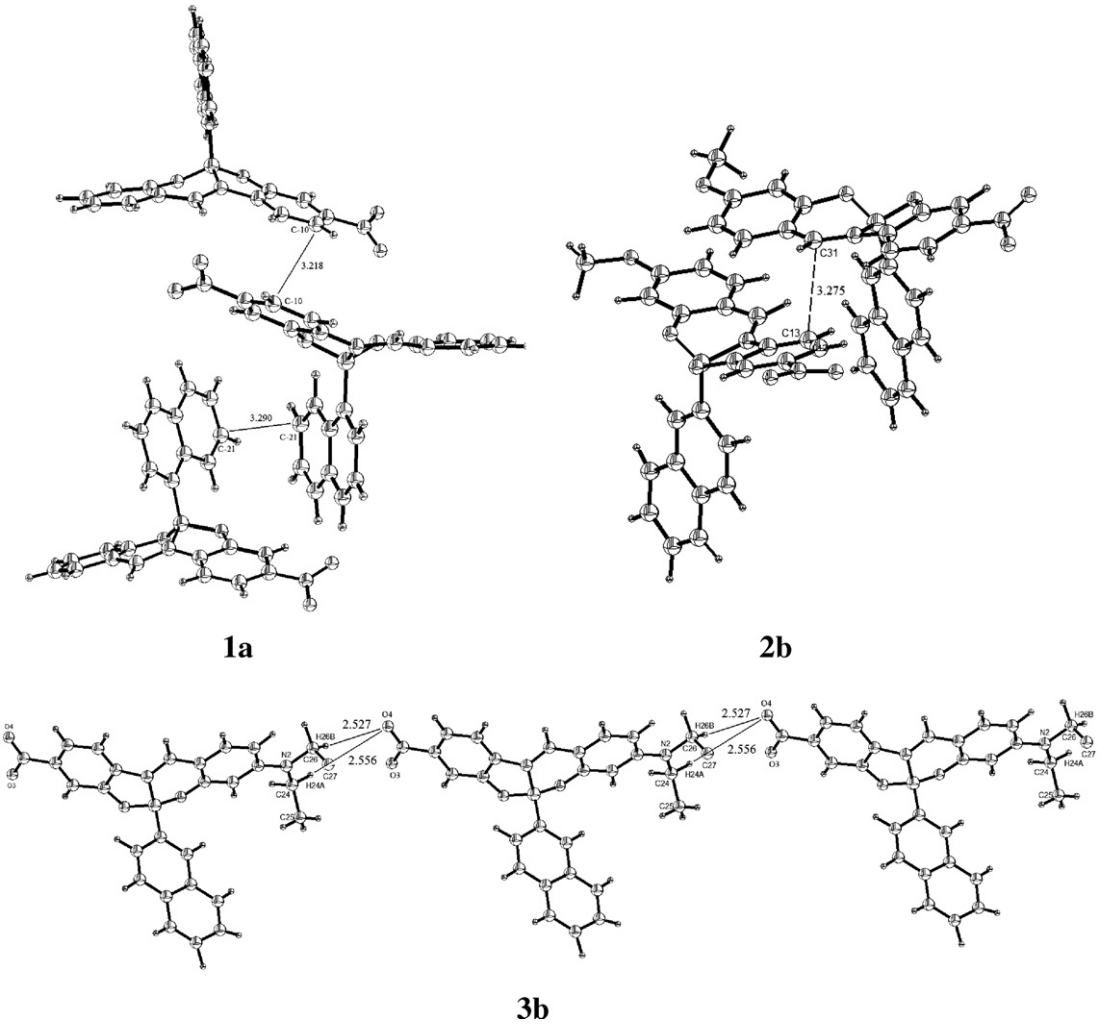

Fig. 8. Intermolecular interaction in the crystal packing of **1a**, **2b** and **3b**.

complex–$N(Et)_2\cdots O_2N$-complex resulting in a head–tail chain (Fig. 8). These contacts are less than the sum of the van der Waals radii ($\sum r_{vdW}$H–O = 2.7 Å) [20]. For molecular materials the π–π stacking interactions and hydrogen bonds might be beneficial in terms of charge transfer [23].

2.4. NLO properties

(a) *Second-order*: the experimental hyperpolarizabilities (β) for compound **1a**, **1b**, **2b**, **2c**, **3a**–**3c**, were measured by the electric field-induced second harmonic (EFISH) technique and the data are shown in Table 5. Attempts to carry out measurements on the ligands were unsuccessful due to their insolubility in chloroform. The data clearly reveals that β is larger for the compound containing the -$N(Et_2)$ group as donor.Except for **2b**, the explanation that NLO effects are ultimately related to the intense charge transfer between electron donating and accepting fragment, is in agreement with the simple, but widely used "2 level" model [24]:

$$\beta_{1\to 2} = \frac{3e^2 f_{1\to 2}\Delta\mu_{1\to 2}}{2mE_{1\to 2}^3} \times \frac{E_{1\to 2}^4}{\left(E_{1\to 2}^2 - (2\hbar\omega)^2\right)\left(E_{1\to 2}^2 - (\hbar\omega)^2\right)} \quad (1)$$

In this model, $E_{1\to 2}$ is the energy of the transition between the ground and the first excited state, $f_{1\to 2}$ (oscillator strength) is its intensity and $\Delta\mu_{1\to 2}$ the change in dipole moment occurring during the transition. Increasing the strength of the donor acceptor substituents usually provide f and $\Delta\mu$ enhancements and reduce the transition energy, which together lead to a larger molecular hyperpolarizability.To provide a rationale for the unexpected behaviour of **2b**, the electronic features have been analysed in the **1a**–**2b**–**3b** series, for which structural data are available. The results and relevant NLO parameters are presented in Table 6, and compared to the experimental studies in Table 5.The main two orbitals involved in the intense and low lying (1 → 2) transitions of the chromophores are compared in Fig. 9. The major differences are observed at the level of the occupied orbitals, which mostly reflect the contribution of the donor fragment to the ground state electron density. Indeed, H (**1a**), MeO (**2b**) and $N(Et)_2$ (**3b**) contribute <0.1%, 8.5%, and 11.3%, respectively, to the electron density of the related orbitals 70, 77, 86, in full agreement with their relative donating strengths. In the case of **2b**, the data gathered in Table 6 reveals the contribution of additional excitations to the low energy 1 → 2 transition, which arise from orbital 69. This orbital is localized on the nitro group, which leads to an unexpected reduction of the charge transfer and finally to a reduction of $\beta_{1\to 2}$. A qualitative picture for the lowering of the charge transfer process is provided in Fig. 10. Although a methoxy group is present in **2b**, it turns out not to be significantly involved in the charge transfer process. By contrast, and despite a lack of strong donor group, an important donating character (black contribution in Fig. 10) seems to be devoted to the conjugated bridge of **1a**, leading to a rather large NLO response.A final discussion has to be conducted on the rather large experimental difference observed between **2b** and **2c** (Table 5). Indeed, while **1a** and **1b** exhibit similar NLO response with experimental $\beta \times \mu$ value around 90×10^{-30} cm^5 esu^{-1} D, and **3a**, **3b**, and **3c** exhibit $\beta \times \mu$ value around 500×10^{-30} cm^5 esu^{-1} D, in agreement with the fact that the aryl-boronated fragment is not engaged in the charge transfer, the large $\beta \times \mu$ difference (59.1 and 137.9×10^{-30} cm^5 esu^{-1} D, for **2b** and **2c**, respectively) is somewhat surprising. Without structural data for **2c**, it is not possible to conclude unambiguously on the origin of this difference. In a previous investigation [12], we have pointed out that short contacts between the aryl fragments and the oxygen atoms of the boron coordination sphere had the potential to lead to significant β enhancement. If hydrogen bonding is possible between O1 and the substituted boronic fragments, one can infer that it should more likely take place in **2c** than in **2b**. However, the change in hyperpolarizability

Table 5
Experimental (EFISH and THG) and computed (ZINDO) data for the boronate derivatives **1a**–**1c**, **2b**–**2c** and **3a**–**3d**

Compounds	Experimental (EFISH) data $\beta \times \mu$ (10^{-30} cm^5 esu^{-1} D)	Computed (ZINDO) data	β_{2level}[a] μ (D)	Experimental (THG) data $\chi^{(3)}$ ($\times 10^{-12}$ esu)[c]
1a	87.9	10.7	12.1	1.55
1b	92.8[b]			1.58
1c				1.42
2b	59.1[b]	4.6	11.0	
2c	137.9			1.10
3a	485.9			4.05
3b	535.0	14.2	18.2	5.07
3c	497.9			5.01
3d				5.67

Compounds **1**, **2**, **3**, **1c** and **2a** were not sufficiently soluble to be measured in EFISH and TGH was not measured for **2b**.
[a] Calculated from Eq. (1).
[b] Measured in a 9:1 $CHCl_3$:DMSO mixture.
[c] $\chi^{(3)}$ for fused silica = 3.1×10^{-14} esu.

Table 6
Low energy transitions and relevant parameters (absorption maxima, oscillator strengths dipole moment changes, and compositions of the configuration interaction), for **1a**, **2b**, and **3b**

Compound	Transitions	λ_{max} (nm)	f	$\Delta\mu$ (D)	Composition of CI expansion
1a	1 → 2	402	0.44	5.0	$\chi_{70\to 73}$ (68%)
2b	1 → 2	412	0.35	2.5	$\chi_{77\to 79}$ (48%)
					$\chi_{69\to 80}$ (15%)
					$\chi_{69\to 79}$ (12%)
3b	1 → 2	434	0.74	2.9	$\chi_{86\to 88}$ (78%)

Orbital 72(73) is the HOMO(LUMO) for **1a**, orbital 78(79) is the HOMO(LUMO) for **2b**, orbital 87(88) is the HOMO(LUMO) for **3b**.

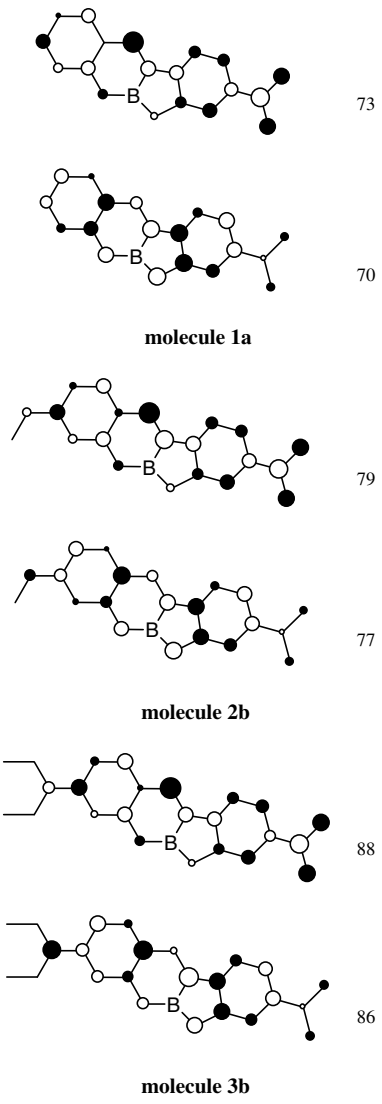

Fig. 9. Main orbitals involved in the charge transfer process for **1a**, **2b**, and **3c**. Orbitals 70(73), 77(79) and 86(88) are occupied (unoccupied) orbitals, defined in Table 6.

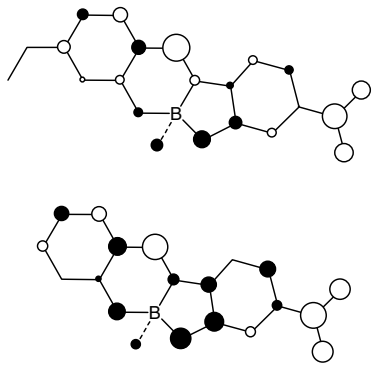

Fig. 10. Comparison of the charge transfer processes in **2b** (top) and **1a** (bottom). White (black) contributions are indicative of increase (decrease) of the electron density upon 1 → 2 transition.

is not observed between **3b** and **3c**, as well. This suggests that an explanation based only on this short contact is probably not fully reliable.

(b) *Third-order*: the cubic non-linear responses for the series **1a**–**3a**, **1b**–**3b**, **1c**–**3c** and **3d** were estimated through the use of third-harmonic generation (THG) Maker-fringes technique [25] exciting at the IR wavelength of 1200 nm. This technique allowed us to calculate the third-order non-linear susceptibility $\chi^{(3)}$ of our boron chromophores dispersed into polymer films. The THG measurements were performed on thin polymer (polystyrene: PS) films doped with the boronates at a loading level of 30 wt.% (weight percent). At this doping level the samples exhibit a third-order non-linear susceptibility of the order $\chi^{(3)} \sim 10^{-12}$ esu. The $\chi^{(3)}$ values for each boronate are summarized in Table 5 (note that for compounds **2a** and **2b**, THG data are not reported since optical quality in polymer films was not acceptable, i.e., they exhibit strong light scattering at the fundamental and harmonic wavelengths). Thus, except for **2c**, our measurements show that there exists a correlation between the quadratic and cubic non-linear responses which are ultimately related to charge transfer transitions involving donor and acceptor substituents. For instance, the largest nonlinearities were observed for the compounds **3a**–**3d** having the very strong donor $N(Et)_2$ group which lead to the highest $\beta \times \mu \sim 500 \times 10^{-30}$ cm^5 esu^{-1} D and $\chi^{(3)} \sim 5 \times 10^{-12}$ esu for the quadratic and cubic cases, respectively. Interestingly, the THG measurements also show that despite a lack of strong donor group in **1a**, **1b** and **1c**, this series exhibit a larger NLO response compared with **2c** which possesses a methoxy group (OMe) with higher donating strength. Unfortunately, for the reasons above mentioned, it was not possible to measure the cubic non-linearity of **2b** to contrast it with the quadratic non-linear behaviour previously discussed. So, depending on the donor group it was found that the films doped with the boronates have a third-order non-linear susceptibility $\chi^{(3)}$ that varied from 35 up to 180 times the values corresponding to the standard reference used in our experiments, i.e., fused silica. It is worth to mention that the choice of using THG as a technique to measure $\chi^{(3)}$ allowed us to measure pure electronic NLO effects at infrared wavelength (important for photonic applications such as high bandwidth all-optical switching).

3. Conclusions

Ten new boronates with H, OMe and $N(Et_2)$ donor groups (series **1a**–**c**, **2a**–**c** and **3a**–**d**, respectively) were synthesized easily in good yields, and the NLO properties were investigated for the first time for both quadratic (EFISH experiments) and cubic (THG Maker-fringes experiments) orders. The X-ray crystal structures show that the stilbene fragments reveal a planar array in the ligands and are bent in the boron complexes. The weak intramolecular interaction for compound **1a** observed in solution was retained in the solid state. The increase of the "α" and "β" angle

can be attributed to the presence of naphthyl groups, which could be used to modulate the electronic properties of the rigid stilbene skeleton, and finally the optical properties of the materials. At the second-order level, the observation of an enhancement of 2–3 times of the NLO response between compounds **2b** and **2c** suggests that the presence of additional bulky π-conjugated substituents (e.g. naphthyl) in the proximity of the charge transfer pathway of push–pull NLO chromophores has the potential to modulate the molecular conformation, the electronic features of the bridge and finally to affect the overall NLO response. Nevertheless, at the third-order level, the NLO modulation induced by a bulky substituent resulted rather weak, though the substitution of electronic donor groups enhanced between 3.5 and 4.5 the non-linear response. The nonlinearities in these kind of molecules, which up to now have received a limited attention, could deserve further investigation in a perspective of developing boron-based non-linear materials with potential applications in photonics.

4. Experimental

4.1. Instrument

All starting materials were purchased from Aldrich. Solvents were used without further purification. Melting points were recorded on a Electrothermal 9200 apparatus and are uncorrected. Infrared spectra were measured on a FT-IR Perkin-Elmer GX spectrophotometer using KBr pellets. ^{1}H, ^{11}B and ^{13}C NMR spectra were recorded on a Bruker avance DPX 300, Jeol GX 270 and Jeol Eclipse +400 spectrometers. Chemical shifts (ppm) are relative to $(CH_3)_4Si$ for ^{1}H and ^{13}C and to $BF_3(OEt_2)$ for ^{11}B. Ultraviolet spectra were obtained with a Perkin–Elmer Lambda 12 spectrophotometer. Mass spectra were recorded on a Hewlett–Packard 5989A spectrometer. Elemental analyses were carried out on a Thermo Finnigan Flash EA 1112 elemental microanalyzer.

4.2. X-ray data collection and structure determination

In all cases the single crystals suitable for X-ray structural studies were obtained by slow evaporation from mixtures of $CHCl_3$ and hexane. The crystal data were recorded on an Enraf Nonius Kappa-CCD (λ Mo $K\alpha = 0.71073$ Å, graphite monochromator, $T = 293$ K-CCD rotating images scan mode). The crystals were mounted on a Lindeman tube. Absorption corrections were performed using the SHELX-A [26] program. All reflection dataset were corrected for Lorentz and polarization effects. The first structure solution was obtained using the SHELXS-97 program and then SHELXL-97 program was applied for refinement and output data [26]. All software manipulations were done under the WIN-GX environment program set [27]. Molecular perspectives were drawn under ORTEP3 drawing application [28]. All heavier atoms were found by Fourier map difference and refined anisotropically. Some hydrogen atoms were found by Fourier map differences and refined isotropically. The remaining hydrogen atoms were geometrically modelled and are not refined.

4.3. NLO measurements

Second-order: the experimental hyperpolarizabilities (β) were investigated by electric field induced second harmonic (EFISH) technique [29,30]. The data were recorder using picosecond Nd:YAG pulsed (10 Hz) laser operating at 1.064 μm. The outcoming Stokes-shifted radiation at 1.907 μm generated by Raman effect in a hydrogen cell (1 m long, 50 bar) was used as the fundamental beam for second harmonic generation (SHG). The centrosymmetry of the solution was broken by dipolar orientation of the chromophores with a high voltage pulse pulse (5 kV) synchronized with the laser pulse. The SHG signal was selected through a suitable interference filter, detected by a photomultiplier, and recorded on a Tektonic TDS 620 oscilloscope.

4.3.1. Theoretical methods

The all-valence INDO (intermediate neglect of differential overlap) method [31], was employed for the calculation of the electronic transitions, to analyze the origin of the charge transfer at the atomic level. Calculations were performed using the INDO/1 Hamiltonian incorporated in the commercially available MSI software package ZINDO [32]. The monoexcited configuration interaction (MECI) approximation was employed to describe the excited states. The 100 lowest energy transitions between the 10 highest occupied molecular orbitals and the 10 lowest unoccupied ones were chosen to undergo CI mixing.

Third-order: these molecules were studied in solid state (solid films) using the guest(molecule)–host(polymer) approach. Ratios of 70:30 wt.% of polystyrene (PS) and boronates **1a**, **2c**, **3a**–**3d** were dissolved in chloroform while **1b**–**1c** were dissolved in tetrahydrofuran. The solid films were deposited on fused silica substrates (1 mm-thick) by using the spin coating technique. The prepared films had typical thickness between 50 and 300 nm with good optical quality showing negligible light scattering at visible and NIR wavelengths. Absorption spectra of spin-coated films were obtained with a spectrophotometer (Perkin–Elmer Lambda 900). Sample thickness was measured by using a Dektak 6 M profiler.

THG Maker-fringes setup is reported elsewhere [33]. Briefly, it consisted of a Nd-YAG laser-pumped optical parametric oscillator (OPO) that delivered pulses of 8 ns at a repetition rate of 10 Hz. A fundamental wavelength of 1200 nm (idler beam) was used. The output of the OPO system was focused into the films with a 30-cm focal-length lens to form a spot with a radius of approximately 150 μm. Typical energies in our measurements were

set at 1 mJ per pulse at sample position (corresponding to peak intensities of ~0.18 GW/cm^2). The third-harmonic beam, as a bulk effect, emerging from the films was separated from the pump beam by using a color filter and detected with a PMT and a Lock-in amplifier. The THG measurements were performed for incident angles in the range from −40° to 40° with steps of 0.27°. All the experiment was computer controlled.

In the Maker-fringes technique, the third-harmonic peak intensity $I^{3\omega}$ from the substrate-film structure is compared to one produce from the substrate alone. Then, the non-linear susceptibility $\chi^{(3)}$ in a film of thickness L_f is determined from [34]:

$$\chi^{(3)} = \chi_s^{(3)} \frac{2}{\pi} \left(\frac{L_{c,s}}{L_f}\right) \left(\frac{I_f^{3\omega}}{I_s^{3\omega}}\right)^{1/2} \quad (2)$$

where $\chi_s^{(3)}$ and $L_{c,s}$ are the non-linear susceptibility and coherence length, respectively, for the substrate at the fundamental wavelength. In our calculation, we considered $\chi_s^{(3)} = 3.1 \times 10^{-14}$ esu and $L_{c,s} = 9$ μm for the fused silica substrate [33]. In any case, our samples satisfied the condition $L_f \ll L_{c,s}$ in which Eq. (2) is valid.

4.4. Syntheses

The following procedure was used in the syntheses of all boron compounds described herein. Equimolecular amounts of 4-diethylaminosalicylaldehyde (4-methoxysalicylaldehyde or salicyladehyde), 2-amino-5-nitrophenol and the corresponding arylboronic or naphthylboronic acids were refluxed in a mixture of acetonitrile and acetic acid (9:1 ratio) for 6–12 h and allowed to cool to room temperature. The solid precipitate was collected by filtration under vacuum and washed with hexane, followed by recrystallization from chloroform–hexane.

4.4.1. 2-(2-Hydroxybenzylideneamino)-5-nitrophenol (*1*)

Compound **1** was obtained from 0.120 g (1.00 mmol) of 2-hydroxybenzaldehyde and 0.150 g (1.00 mmol) de 2-amino-5-nitrophenol. The product was obtained as a red solid (0.190 g), yield 74%, m.p. 216–218 °C. UV/Vis ($CHCl_3$); λ_{max}(nm) (ε): 375 (76489). The spectroscopic characterization has been previously reported [15].

4.4.2. 2-(1-Naphthyl-(3′-nitrobenzo[d]))-1,3-dioxa-6-aza-2- boracyclonon-6-ene (*1a*)

Compound **1a** was obtained from 0.120 g (1.00 mmol) of 2-hydroxybenzaldehyde, 0.150 g (1.00 mmol) of 2-amino-5-nitrophenol and 0.170 g (1.00 mmol) af 1-naphthylboronic acid. The product was obtained as an orange solid (0.320 g), yield 81%, m.p. 150–152 °C. IR (KBr) ν_{max} (cm^{-1}): 3397, 3055, 2250, 1629 (C=N), 1588, 1545, 1520, 1463, 1381, 1341, 1293, 1261, 1154, 1125, 1070, 1042, 997. UV/Vis ($CHCl_3$); λ_{max}(nm) (ε): 456 (11700). MS *m/z* (%): 394 (M^+, 65), 364 (3), 267 (100), 221 (50); ^{1}H NMR (400 MHz, $CDCl_3$) δ (ppm): 6.94 (1H, dt, $J = 7.6$, 0.9 H-5), 7.02–7.05 (2H, m, H-3, H-17), 7.16 (1H, t, $J = 8.0$ Hz, H-16), 7.45–7.52 (4H, m, H-4, H-6, H-13, H-20), 7.61 (1H, t, $J = 7.9$ Hz, H-21), 7.66 (1H, dd, $J = 1.9$, 8.0 Hz, H-15), 7.77 (1H, d, $J = 7.9$ Hz, H-19), 7.80 (1H, d, $J = 2.2$ Hz, H-10), 7.83 (1H, dd, $J = 2.2$, 8.8 Hz, H-12), 8.77 (1H, s, H-7), 8.82 (1H, d, $J = 7.9$ Hz, H-22); ^{13}C NMR (100 MHz, $CDCl_3$) δ (ppm): 110.8 (C-10), 114.8 (C-13), 115.1 (C-12), 119.3 (C-1), 120.9 (C-3), 121.0 (C-5), 124.6 (C-16), 125.4 (C-20), 125.6 (C-21), 128.4 (C-19), 128.5 (C-15), 128.9 (C-17), 129.5 (C-22), 132.0 (C-6), 133.9 (C-18), 135.5 (C-23), 135.6 (C-11), 139.7 (C-4), 149.9 (C-8), 152.7 (C-7), 157.7 (C-9), 158.3 (C-2); ^{11}B NMR (96 MHz, $CDCl_3$) δ (ppm): +9.79 ($h_{1/2}$ = 192 Hz); Elemental Anal. Calc. for $C_{23}H_{15}O_4N_2$-B–C_2H_3N: C, 68.99; H, 4.17; N, 9.65. Found: C, 68.51; H, 4.20; N, 9.17%.

4.4.3. 2-(2-Naphthyl-(3′-nitrobenzo[d]))-1,3-dioxa-6-aza-2-boracyclonon-6-ene (*1b*)

Compound **1b** was obtained from 0.120 g (1.00 mmol) of 2-hydroxybenzaldehyde, 0.150 g (1.00 mmol) of 2-amino-5-nitrophenol and 0.170 g (1.00 mmol) of 2-naphthylboronic acid. The product was obtained as a yellow solid (0.350 g), yield 87%, m.p. 140–142 °C. IR (KBr) ν_{max} (cm^{-1}): 3382, 3321, 3109, 3052, 1626 (C=N), 1546, 1524, 1467, 1378, 1338, 1293, 1263, 1227, 1155, 1122, 1065, 977, 934, 867, 821 753. UV/Vis ($CHCl_3$); λ_{max} (nm) (ε): 462 (4870). MS *m/z* (%): 395 (M^++1, 25), 394 (M^+, 86), 393 (30), 364 (4), 267 (100), 221 (61) 127 (6); ^{1}H NMR (400 MHz, $CDCl_3$) δ (ppm): 7.02 (1H, t, $J = 7.5$ Hz, H-5), 7.29 (1H, d, $J = 8.4$ Hz, H-3), 7.34–7.42 (3H, m, H-15, H-18, H-21), 7.48 (1H, d, $J = 7.5$ Hz, H-6), 7.58 (1H, d, $J = 8.6$ Hz, H-13), 7.63–7.72 (4H, m, H-4, H-16, H-19, H-20), 7.74 (1H, s, H-23), 7.86 (1H, dd, $J = 2.0$, 8.6 Hz, H-12), 7.93 (1H, d, $J = 2.0$ Hz, H-10), 8.55 (1H, s, H-7); ^{13}C NMR (75 ^{13}C MHz, $CDCl_3$) δ (ppm): 110.7 (C-10), 115.4 (C-13), 115.6 (C-12), 119.4 (C-1), 121.1 (C-3), 121.5 (C-5), 125.9 (C-21), 126.1 (C-18), 127.4 (C-16), 127.9 (C-20), 128.4 (C-19), 128.9 (C-15), 131.2 (C-23) 132.7 (C-6), 133.2 (C-17), 133.9 (C-22), 136.2 (C-11), 140.4 (C-4), 150.3 (C-8), 152.9 (C-7), 158.7 (C-9), 159.0 (C-2); ^{11}B NMR (128 MHz, $CDCl_3$) δ (ppm): +8.61 ($h_{1/2}$ = 128 Hz).

4.4.4. 2-(2-Methylbenzo-(3-nitrobenzo[d]))-(benzo[h]-1,3-dioxa-6-aza-2-boracyclonon-6-ene (*1c*)

Compound **1c** was obtained from 0.120 g (1.00 mmol) of 2-hydroxybenzaldehyde, 0.150 g (1.00 mmol) of 2-amino-5-nitrophenol and 0.130 g (1.00 mmol) of *o*-tolylboronic acid. The product was obtained as an orange solid (0.320 g), yield 89%, m.p. 204–206 °C. IR (KBr) ν_{max} (cm^{-1}): 3392, 3216, 3063, 1617 (C=N), 1585, 1542, 1464, 1379, 1338, 1263, 1179, 1064, 995, 953, 872, 819, 754, 754. MS *m/z* (%): 357 (M^++1, 3), 358 (M^+, 10), 267 (100), 237 (25), 221 (38); ^{1}H NMR (300 MHz, $CDCl_3$) δ (ppm): 2.72 (3H, s, CH_3), 6.89–6.94 (2H, m, H-6, H-16), 6.98 (1H, t, $J = 7.2$ Hz, H-5), 7.07–7.16 (3H, m, H-3,

H-17, H-18), 7.52 (1H, d,$J = 8.0$ Hz, H-19), 7.57 (1H, t, $J = 7.2$ Hz, H-4), 7.65 (1H, d, $J = 8.4$ Hz, H-13), 7.82–7.85 (2H, m, H-10, H-12), 8.73 (1H, s, H-7); ^{13}C NMR (75 MHz, $CDCl_3$) δ (ppm): 22.2 (CH_3), 110.9 (C-10), 114.8 (C-13), 115.2 (C-12), 119.4 (C-1), 120.9 (C-3), 121.2 (C-5), 124.2 (C-16), 128.0 (C-18), 130.4 (C-17), 131.2 (C-6), 132.6 (C-19), 135.8 (C-15) 139.9 (C-4), 141.8 (C-11), 150.0 (C-8), 152.5 (C-7), 157.8 (C-9), 158.4 (C-2); ^{11}B NMR (96 MHz, $CDCl_3$) δ (ppm): +9.3 ($h_{1/2} = 192.6$ Hz). Elemental Anal. Calc. for $C_{20}H_{15}BN_2O_4$ C, 67.07; H, 4.22; N, 7.82. Found: C, 66.63; H, 4.25; N, 7.85. HRMS calcd m/z for $C_{20}H_{15}BN_2O_4[M^+ + H]^+$: 359.1197; Found: 359.1202 error 1.2 ppm.

4.4.5. 2-(2-Hydroxy-4-methoxybenzylideneamino)-5-nitrophenol (**2**)

Compound **2** was obtained from 0.150 g (1.00 mmol) of 2-hydroxy-4-methoxy-benzaldehyde and 0.150 g (1.00 mmol) of 2-amino-5-nitrophenol. The product was obtained as an orange solid (0.270 g), yield 94%, m.p. 232-234 °C. IR (KBr) ν_{max} (cm^{-1}): 3431(OH), 2979, 2895, 2470, 1620 (C=N), 1583, 1513, 1458, 1332, 1238, 1142, 1074, 947, 867, 811, 783, 741. UV/Vis ($CHCl_3$); λ_{max}(nm)(ε): 376 (71215). MS m/z (%): 289 (M^++1, 18), 288 (M^+, 100), 271 (11), 241 (24), 199 (7), 165(6), 151 (9), 124 (14), 78 (4); ^{1}H NMR (400 MHz, DMSO-d_6) δ (ppm): 3.78 (3H, s, OCH_3), 6.36 (1H, d, $J = 2.2$ Hz, H-3), 6.45 (1H, dd, $J = 2.2$, 8.8 Hz, H-5), 7.45 (1H, d, $J = 8.8$ Hz, H-6), 7.48 (1H, d, $J = 8.8$ Hz, H-13), 7.62 (1H, d $J = 2.2$, 8.8 Hz, H-12), 7.66 (1H, d, $J = 2.2$ Hz, H-10), 8.97 (1H, s, H-7); ^{13}C NMR (68 MHz, DMSO-d_6) δ (ppm): 56.0 (OMe), 101.6 (C-3), 107.8 (C-5), 111.4 (C-10), 113.6 (C-1), 114.7 (C-12), 120.1 (C-13), 134.9 (C-6), 141.4 (C-8), 145.9 (C-11), 152.6 (C-9), 162.5 (C-7), 165.2 (C-2), 166.8 (C-4). Elemental Anal. Calc. for $C_{14}H_{12}N_2O_5$ C, 58.33; H, 4.19; N, 9.71. Found: C, 58.99; H, 4.27; N, 10.03%. HRMS calcd m/z for $C_{14}H_{12}N_2O_5$ $[M^+ + H]^+$: 289.0818; Found: 289.0821 error 0.7 ppm.

4.4.6. 2-(1-Naphthyl-(3′-nitrobenzo[d]))-(4″- methoxybenzo[h])-1,3-dioxa-6-aza-2-boracyclonon-6-ene (**2a**)

Compound **2a** was obtained from 0.150 g (1.00 mmol) of 2-hydroxy-4-methoxy-benzaldehyde, 0.150 g (1.00 mmol) of 2-amino-5-nitrophenol and 0.170 g (1.00 mmol) of 1-naphthylboronic acid. The product was obtained as an orange solid (0.270 g), yield 64%, m.p. 260-262 °C. IR (KBr) ν_{max} (cm^{-1}): 3040, 2945, 2843, 1608 (C=N), 1582, 1527, 1469, 1382, 1337, 1293, 1234, 1171, 1121, 1069, 1042, 1021, 964, 934, 875, 819, 801, 782. UV/Vis ($CHCl_3$); λ_{max}(nm) (ε): 460 (8740). MS m/z (%): 425 ($M^+ + 1$, 1) 424 (M^+, 6), 297 (100), 267 (16), 251 (44), 208 (11), 127 (8); ^{1}H NMR (400 MHz, $CDCl_3$) δ (ppm): 3.75 (3H, s, OCH_3), 6.42 (1H, d, $J = 2.2$ Hz, H-3), 6.49 (1H, dd,$J = 2.2$, 8.8 Hz, H-5), 7.05 (1H, d,$J = 6.9$ Hz, H-17), 7.19 (1H, t, $J = 6.9$ Hz, H-16), 7.37 (1H, d, $J = 8.8$ Hz, H-6), 7.47 (1H, t, $J = 7.0$ Hz, H-20), 7.54 (1H, d, $J = 8.4$, H-13), 7.61 (1H, t, $J = 7.0$ Hz, H-21), 7.67 (1H, d, $J = 6.9$ Hz, H-15), 7.75 (1H, d, $J = 2.2$ Hz, H-10), 7.78 (1H, d, $J = 7.0$ Hz, H-19), 7.80 (1H, dd, $J = 2.2$, 8.4 Hz, H-12), 8.60 (1H, s, H-7), 8.81 (1H, d, $J = 7.7$ Hz, H-22); ^{13}C NMR (100 MHz, $CDCl_3$) δ (ppm): 56.0 (OCH_3), 102.9 (C-3), 110.4 (C-10), 111.8 (C-5), 113.4 (C-1), 113.8 (C-13), 115.2 (C-12), 124.6 (C-16), 125.3 (C-20), 125.5 (C-21), 128.3 (C-15), 128.4 (C-19), 128.8 (C-17), 129.5 (C-22), 133.4 (C-6), 133.9 (C-18), 135.5 (C-23), 136.3 (C-11), 149.1 (C-8), 151.3 (C-7), 157.6 (C-9), 161.1 (C-2), 169.8 (C-4); ^{11}B NMR (128 MHz, $CDCl_3$) δ (ppm): +9.77 ($h_{1/2} = 64$ Hz). Elemental Anal. Calc. for $C_{24}H_{17}BN_2O_5$ C, 67.95; H, 4.04; N, 6.60. Found: C, 67.46; H, 4.15; N, 6.83%. HRMS calcd m/z for $C_{24}H_{17}BN_2O_5$ $[M^+ + H]^+$: 425.1303; Found: 425.1306 error 0.6 ppm.

4.4.7. 2-(2-Naphthyl-(3′-nitrobenzo[d]))-(4″-methoxybenzo[h])-1,3-dioxa-6-aza-2-boracyclonon-6-ene (**2b**)

Compound **2b** was obtained from 0.150 g (1.00 mmol) of 2-hydroxy-4-methoxy-benzaldehyde, 0.150 g (1.00 mmol) of 2-amino-5-nitrophenol and 0.170 g (1.00 mmol) of 2-naphthylboronic acid. The product was obtained as an orange solid (0.370 g), yield 87%, m.p. 220–222 °C. IR (KBr) ν_{max} (cm^{-1}): 3041, 2927, 2842, 1606 (C=N), 1582, 1528, 1384, 1337, 1293, 1234, 1170, 1122, 1067, 1042, 1021, 966, 933, 875, 820, 800, 782. UV/Vis ($CHCl_3$); λ_{max} (nm) (ε): 461 (22100). MS m/z (%): 425 (M^++1, 9), 424 (M^+, 34), 297 (100), 267 (10), 251 (67); 127 (3); ^{1}H NMR (400 MHz, $CDCl_3$) δ (ppm): 3.65 (3H, s, OMe), 6.31 (1H, dd, $J = 2.2$, 8.8 Hz, H-5), 6.41 (1H, d, $J = 2.2$ Hz, H-3), 7.03–7.07 (2H, m, H-18, H-21), 7.12 (1H, d, $J = 8.0$ Hz, H-15), 7.19 (1H, d, $J = 8.8$ Hz, H-6), 7.33 (1H, d, $J = 8.0$, Hz, H-16), 7.36-7.44 (2H, m, H-19, H-20), 7.44 (1H, s, H-23), 7.47 (1H, d, $J = 8.7$ Hz, H-13), 7.52 (1H, d, $J = 2.2$ Hz, H-10), 7.56 (1H, dd, $J = 2.2$, 8.7 Hz, H-12), 8.63 (1H, s, H-7); ^{13}C NMR (100 MHz, DMSO-d_6) δ (ppm): 56.0 (OMe), 102.6 (C-3), 109.0 (C-10), 110.9 (C-5), 113.4 (C-1), 115.0 (C-13), 115.2 (C-12), 125.3, 125.4 (C-18, C-21), 126.7 (C-16), 127.3, 127.8 (C-20, C-19), 128.6 (C-15), 130.2 (C-23), 132.7 (C-17), 133.2 (C-22), 134.2 (C-6), 136.9 (C-11), 148.6 (C-8), 153.0 (C-7), 157.5 (C-9), 161.0 (C-2), 169.6 (C-4); ^{11}B NMR (128 MHz, DMSO-d_6) δ (ppm): +8.0 ($h_{1/2} = 320$ Hz). Elemental Anal. Calc. for $C_{24}H_{17}O_5N_2B$: C, 67.98; H, 4.01; N, 6.60. Found: C, 67.21; H, 4.18; N, 6.49%. HRMS calcd m/z for $C_{24}H_{17}BN_2O_5$ $[M^+ + H]^+$: 425.1303; Found: 425.1303 error 0.07 ppm.

4.4.8. 2-(2-Methylbenzo-(3-nitrobenzo[d]))-(methoxybenzo[h])-1,3-dioxa-6-aza-2-boracyclonon-6-ene (**2c**)

Compound **2c** was obtained from 0.150 g (1.00 mmol) of 2-hydroxy-4-methoxy-benzaldehyde, 0.150 g (1.00 mmol) of 2-amino-5-nitrophenol and 0.130 g (1.00 mmol) of *o*-tolylboronic acid. The product was obtained as an orange solid (0.250 g), yield 65%, m.p. 230–232 °C. IR (KBr) ν_{max} (cm^{-1}): 2928, 1613 (C=N), 1582, 1529, 1471, 1385, 1335,

1299, 1237, 1171, 1139, 1062, 1022, 963, 870, 818, 752, 731. UV/Vis ($CHCl_3$); λ_{max}(nm) (ε): 461 (22800). MS *m/z* (%): 388 (M^+, 3), 297 (100), 267(5), 251 (47), 208 (14), 91(5); ^{1}H NMR (270 MHz, $CDCl_3$) δ (ppm): 2.68 (3H, s, CH_3), 3.83 (3H, s, OCH_3), 6.49 (1H, d, $J = 2.4$ Hz, H-3), 6.52 (1H, dd, $J = 8.4$, 2.4 Hz, H-5), 6.87–6.95 (2H, m, H-16, H-19), 7.05–7.10 (2H, m, H-17, H-18), 7.36 (1H, d, $J = 8.4$ Hz, H-6), 7.52 (1H, d, $J = 8.4$ Hz, H-13), 7.76 (1H, d, $J = 2.2$, Hz, H-10), 7.79 (1H, dd, $J = 8.4$, 2.2 Hz, H-12), 8.55 (1H, s, H-7); ^{13}C NMR (75 MHz, $CDCl_3$) δ (ppm): 22.3 (CH_3), 56.2 (OCH_3), 102.9 (C-3), 110.5 (C-10), 111.8 (C-5), 113.6 (C-1), 113.9 (C-13), 115.2 (C-12), 124.2 (C-16), 127.9 (C-18), 130.4 (C-17), 131.2 (C-19), 133.7 (C-6), 136.5 (C-15), 141.8 (C-11), 149.1 (C-8), 151.2 (C-7), 157.7 (C-9), 161.1 (C-2), 169.9 (C-4); ^{11}B NMR (96 MHz, $CDCl_3$) δ (ppm): +9.17 ($h_{1/2} = 193$ Hz). Elemental Anal. Calc. for $C_{21}H_{17}O_5N_2B$: C, 64.98; H, 4.41; N, 7.22. Found: C, 65.43; H, 4.12; N, 7.01%. HRMS calcd *m/z* for $C_{21}H_{17}O_5N_2B$ $[M^+ + H]^+$: 389.1303; Found 389.1308 error 1.2 ppm.

4.4.9. 2-4-(Diethylamino-2-hydroxybenzylideneamino)-5- nitrophenol (3)

Compound **3** was obtained from 0.190 g (1.00 mmol) of 4-(diethylamino)-salicylaldehyde and 0.150 g (1.00 mmol) of 2-amino-5-nitrophenol. The product was obtained as a red solid (0.230 g), yield 69%, m.p. 254–256 °C. IR (KBr) ν_{max} (cm^{-1}): 3436, 2938, 1619 (C=N), 1586, 1523, 1397, 1339, 1230, 1124, 1073, 1017, 945. UV/Vis ($CHCl_3$); λ_{max}(nm) (ε): 436 (89920). MS *m/z* (%): 329 (M^+, 97), 314 (100), 300 (14), 286 (8); ^{1}H NMR (400 MHz, DMSO-d_6) δ (ppm): 1.12 (6 H, t, CH_3), 3.39 (4H, q, N–CH_2), 5.94 (1H, d, $J = 2.2$ Hz, H-3), 6.32 (1H, dd, $J = 2.2$, 8.8 Hz, H-5), 7.27 (1H, d, $J = 8.8$ Hz, H-6), 7.46 (1H, d, $J = 8.4$ Hz, H-13), 7.62–7.64 (2H, m, H-10, H-12), 8.77 (1H, s, H-7), ^{13}C NMR (68 MHz, DMSO-d_6) δ (ppm): 12.7 (Me), 44.7 (CH_2–N), 98.4 (C-3), 104.8 (C-5), 110.3 (C-10), 111.2 (C-12), 111.9 (C-1), 119.2 (C-13), 135.2 (C-6), 141.6 (C-8), 145.8 (C-11), 153.2 (C-9), 156.8 (C-7), 159.1 (C-4), 168.9 (C-2). HRMS calcd *m/z* for $C_{17}H_{19}N_3O_4$ $[M^+ + H]^+$: 330.1448; Found 330.1451 error 0.8 ppm.

4.4.10. 2-(1-Naphthyl-(3′-nitrobenzo[d]))-(4″- diethylaminobenzo[h])-1,3-dioxa-6-aza-2-boracyclonon-6-ene (3a)

Compound **3a** was obtained from 0.190 g (1.00 mmol) of 4-diethylaminesalicylaldehyde, 0.150 g (1.00 mmol) of 2-amino-5-nitrophenol and 0.170 g (1.00 mmol) of 1-naphthylboronic acid. The product was obtained as a red solid (0.410 g), yield 88%, m.p. 238–240 °C. IR (KBr) ν_{max} (cm^{-1}): 3037, 2972, 2930, 2380, 1606 (C=N), 1572, 1526, 1446, 1418, 1375, 1328, 1244, 1185, 1135, 1063, 1039, 959, 932, 862, 819, 788. UV/Vis ($CHCl_3$); λ_{max}(nm) (ε): 506 (34060). MS *m/z* (%): 466 (M^++1, 7) 465 (M^+, 23), 338 (100), 308 (16), 292 (30), 248 (15), 220(3), 127 (5); ^{1}H NMR (400 MHz, $CDCl_3$) δ (ppm): 1.12 (3H, t, $J = 7.1$, CH_3), 3.32 (4H, m, N–CH_2), 6.06 (1H, d, $J = 2.4$ Hz, H-3), 6.27 (1H, dd, $J = 9.2$, 2.4 Hz, H-5), 7.11 (1H, d, $J = 7.4$ Hz, H-17), 7.19 (1H, t, $J = 7.4$ Hz, H-16), 7.21 (1H, d, $J = 9.2$ Hz, H-6), 7.35 (1H, d, $J = 8.6$, Hz, H-13), 7.45 (1H, t, $J = 7.8$ Hz, H-20), 7.58 (1H, t, $J = 7.8$ Hz, H-21), 7.65 (1H, d, $J = 7.4$ Hz, H-15), 7.69 (1H, d, $J = 2.2$ Hz, H-10), 7.76 (1H, dd, $J = 8.6$, 2.2 Hz, H-12), 7.77 (1H, d, $J = 7.8$ Hz, H-19), 8.34 (1H, s, H-7), 8.84 (1H, d, $J = 7.8$ Hz, H-22); ^{13}C NMR (100 MHz, $CDCl_3$) δ (ppm): 12.8 (CH_3), 45.2 (N–CH_2), 99.4 (C-3), 107.8 (C-5), 109.6 (C-10), 110.6 (C-1), 112.1 (C-13), 115.3 (C-12), 124.7 (C-16), 125.1 (C-20), 125.3 (C-21), 127.9 (C-15), 128.3 (C-19), 128.7 (C-17), 129.8 (C-22), 133.9 (C-18), 134.2 (C-6), 135.7 (C-23), 138.9 (C-18), 147.5 (C-8), 148.4 (C-7), 156.9 (C-9), 157.1 (C-4), 160.5 (C-2); ^{11}B NMR (128 MHz, $CDCl_3$) δ (ppm): +9.5 ($h_{1/2} =$ 256, Hz); Elemental analysis Calc. for $C_{27}H_{24}O_4N_3B$: C, 69.74; H, 5.16; N, 9.03. Found: C, 69.51; H, 5.77; N, 8.87%.

4.4.11. 2-(2-Naphthyl-(3′-nitrobenzo[d]))-(4″- diethylaminobenzo[h])-1,3-dioxa-6-aza-2-boracyclonon-6-ene (3b)

Compound **3b** was obtained from 0.190 g (1.00 mmol) of 4-diethylaminosalicylaldehyde, 0.150 g (1.00 mmol) of 2-amino-5-nitrophenol and 0.170 g (1.00 mmol) of 2-naphthylboronic acid. The product was obtained as a red solid (0.250 g), yield 54%, m.p. 198–200 °C. IR (KBr) ν_{max} (cm^{-1}): 3045, 2974, 1606 (C=N), 1573, 1526, 1448, 1420, 1331, 1246, 1187, 1139, 1067, 959, 932, 866, 821, 745. UV/Vis ($CHCl_3$); λ_{max}(nm) (ε): 511 (63900). MS *m/z* (%): 466 (M^++1, 6), 465 (M^+, 18), 338 (100), 308 (10), 292 (31), 248 (15), 220 (3), 127 (10); ^{1}H NMR (400 MHz, $CDCl_3$) δ (ppm): 1.25 (6H, t, CH_3), 3.46 (4H, m, N–CH_2), 6.33 (1H, dd, $J = 9.5$, 2.6 Hz, H-5) 7.35 (IH, d, $J = 2.6$ Hz, H-3), 7.18 (1H, d, $J = 9.5$ Hz, H-6), 7.29 (1H, d, $J = 8.6$ Hz, H-13), 7.33–7.36 (2H, BB′, H-18, H-21), 7.49 (1H, d, $J = 8.4$ Hz, H-15), 7.66 (1H, d, $J = 8.4$ Hz, H-16), 7.69–7.71 (2H, AA′, H-19, H-20), 7.79 (1H, dd, $J = 2.2$, 8.6 Hz, H-12), 7.81 (1H, s, H-23), 7.83 (1H, d, $J = 2.2$ Hz, H-10), 8.15 (1H, s, H-7); ^{13}C NMR (75 MHz, $CDCl_3$) δ (ppm): 31.2 (N–CH_2), 45.5 (CH_3), 99.3 (C-3), 107.8 (C-5), 109.1 (C-10), 110.5 (C-1), 112.5 (C-13), 115.6 (C-12), 125.4 (C-18, C-21), 126.9 (C-16), 127.7 (C-19), 128.2 (C-20), 129.1 (C-15), 130.5 (C-23), 133.1 (C-17), 133.5 (C-22), 134.6 (C-6) 138.4 (C-11), 147.5 (C-8), 148.6 (C-7), 157.1 (C-9), 157.5 (C-2), 161.1 (C-4); ^{11}B NMR (128 MHz, $CDCl_3$) δ (ppm): +8.3 ($h_{1/2} = 128$ Hz); Elemental Anal. Calc. for $C_{27}H_{24}O_4N_3B$: C, 69.69; H, 5.2; N, 9.03. Found: C, 69.38; H, 5.08; N, 8.89%.

4.4.12. 2-(2-Methylbenzo-(3-nitrobenzo[d]))-(diethylaminobenzo[h])-1,3-dioxa-6-aza-2-boracyclonon-6-ene (3c)

Compound **3c** was obtained from 0.190 g (1.00 mmol) of 4-diethylaminosalicylaldehyde, 0.150 g (1.00 mmol) of 2-amino-5-nitrophenol and 0.130 g (1.00 mmol) of *o*-tolylboronic acid. The product was obtained as a red solid

(0.420 g), yield 90%, m.p. 126–128 °C. IR (KBr) ν_{max} (cm^{-1}): 3109, 2975, 1607 (C=N), 1573, 1526, 1448, 1419, 1377, 1331, 1245, 1185, 1138, 1065, 1012, 960, 932, 857, 818, 787, 749, 729. UV/Vis ($CHCl_3$); λ_{max} (nm) (ε): 490 (16990). MS *m/z* (%): 430 (M^++1, 3), 429 (M^+, 11), 338 (100), 308 (13), 292 (31), 264 (6), 248 (17) 220 (3); ^{1}H NMR (300 MHz, $CDCl_3$) δ (ppm): 1.22 (6H, t, CH_3), 2.71 (3H, s, CH_3), 3.32–3.53 (4H, m, N–CH_2), 6.17 (1H, d, $J = 2.4$ Hz, H-3), 6.32 (1H, dd, $J = 9.2$, 2.4 Hz, H-5), 6.93 (1H, t, $J = 7.0$ Hz, H-16), 7.00 (1H, d, $J = 7.0$ Hz, H-17), 7.08 (1H, dd, $J = 7.0$, 1.7 Hz, H-18), 7.14 (1H, d, $J = 7.0$ Hz, H-19), 7.23 (1H, d, $J = 9.2$ Hz, H-6), 7.38 (1H, d, $J = 8.6$ Hz, H-13), 7.72 (1H, d, $J = 2.2$, Hz, H-10), 7.78 (1H, dd, $J = 8.6$, 2.2 Hz, H-12), 8.33 (1H, s, H-7); ^{13}C NMR (75 MHz, $CDCl_3$) δ (ppm): 12.8 (CH_3), 22.4 (CH_3), 45.4 (N–CH_2), 99.3 (C-3), 107.9 (C-5), 109.5 (C-10), 110.8 (C-1), 112.2 (C-13), 115.3 (C-12), 124.1 (C-17), 127.5 (C-19), 130.2 (C-18), 131.3 (C-16), 134.4 (C-6), 138.1 (C-15), 141.9 (C-11) 147.5 (C-8), 148.5 (C-7), 157.0 (C-9), 157.1 (C-2), 160.6 (C-4); ^{11}B NMR (96 MHz, $CDCl_3$) δ (ppm): +9.1 ($h_{1/2} = 202$ Hz). HRMS calcd *m/z* for $C_{24}H_{24}BN_3O_4$ $[M^+ + H]^+$: 430.1932; Found: 430.1937 error 0.2 ppm.

*4.4.13. 2-(2-Formylbenzo-(3-nitrobenzo[d]))-(diethylaminobenzo[h])-1,3-dioxa-6-aza-2-boracyclonon-6-ene (**3d**)*

Compound **3d** was obtained from 0.140 g (0.44 mmol) of **3** and 0.070 g (0.44 mmol) of *o*-formylboronic acid. The product was obtained as a red solid (0.170 g), yield 87%, m.p. 246–248 °C. IR (KBr) ν_{max} (cm^{-1}): 3123, 2975, 1686, 1607 (C=N), 1574, 1526, 1448, 1420, 1380, 1332, 1246, 1187, 1138, 1066, 963, 934, 857, 779. UV/Vis ($CHCl_3$); λ_{max} (nm) (ε): 484 (30200). MS *m/z* (%): 444 (M^++1, 1), 443 (M^+, 4), 338 (100), 308 (3), 292 (19), 248 (1); ^{1}H NMR (400 MHz, $CDCl_3$) δ (ppm): 1.18 (6H, t, CH_3), 3.31–3.46 (4H, m, N–CH_2), 6.08 (1H, d, $J = 2.4$ Hz, H-3), 6.32 (1H, dd, $J = 9.2$, 2.4 Hz, H-5), 7.11 (1H, dd, $J = 6.3$, 2.2 Hz, H-19), 7.24 (1H, $J = 9.2$ Hz, H-6), 7.26–7.28 (2H, m, H-17, H-18), 7.39 (1H, d, $J = 8.6$ Hz, H-13), 7.68 (1H, d, $J = 2.2$ Hz, H-10), 7.77 (1H, dd, $J = 8.6$, 2.2 Hz, H-12), 7.97 (1H, dd, $J = 6.2$, 2.7 Hz, H-16), 8.39 (1H, s, H-7), 10.94 (1H, s, HCO); ^{13}C NMR (100 MHz, $CDCl_3$) δ (ppm): 12.8 (CH_3), 45.4 (N–CH_2), 99.2 (C-3), 108.2 (C-5), 109.4 (C-10), 110.6 (C-1), 112.1 (C-13), 115.6 (C-12), 127.1 (C-16), 127.7 (C-17), 131.7 (C-19), 132.3 (C-18), 134.4 (C-6), 137.7 (C-15), 139.6 (C-11) 147.4 (C-8), 148.7 (C-7), 156.4 (C-9), 157.2 (C-2), 160.0 (C-4), 196.3 (COH); ^{11}B NMR (128 MHz, $CDCl_3$) δ (ppm): +8.8 ($h_{1/2} = 256$ Hz). HRMS calcd *m/z* for $C_{24}H_{22}BN_3O_5$ $[M^+ + H]^+$: 444.1725; Found 444.1727 error 0.4 ppm.

5. Supplementary material

CCDC 648159, 648160 and 648161 contains the supplementary crystallographic data for this paper. These data can be obtained free of charge from The Cambridge Crystallographic Data Centre via www.ccdc.cam.ac.uk/data_request/cif.

Acknowledgements

The authors thank the UNAM (PAPIIT IN-203207) and CONACyT-CNRS for financial support and the scholarship to B.M. Muñoz, and the ENS Cachan, International Scholarship Program. We also thank M. Leyva for X-ray diffraction and V. González and G. Uribe for NMR spectra.

References

[1] M.F. Hawthorne, M.W. Lee, J. Neurooncol. 62 (2003) 3.
[2] (a) N. Farfán, H. Höpfl, V. Barba, M.E. Ochoa, R. Santillan, E. Gómez, A. Gutiérrez, J. Orgamet. Chem. 581 (1990) 70;
(b) H. Höpfl, M. Sánchez, N. Farfán, V. Barba, Can. J. Chem. 76 (1998) 1352;
(c) N. Christinat, R. Scopelliti, K. Severin, J. Org. Chem. 72 (2007) 2192;
(d) W. Niu, B. Rambo, M.D. Smith, J.J. Lavigne, Chem. Commun. (2005) 5166;
(e) J.L.C. Rowsell, A.R. Millward, K.S. Park, O.M. Yaghi, J. Am. Chem. Soc. 126 (2004) 126.
[3] (a) C. Branger, M. Lequan, R.M. Lequan, M. Barkazoukas, A. Fort, J. Mater. Chem. 6 (1996) 555;
(b) Z. Yuang, N.J. Taylor, T.B. Marder, I.D. Williams, S.K. Kurtz, L.T. Cheng, J. Chem. Soc. Chem. Comm. (1990) 1489.
[4] (a) S.J. Rettig, J. Trotter, Can. J. Chem. 53 (1957) 1393;
(b) N. Farfán, P. Joseph-Nathan, L.M. Chiquete, R. Contreras, J. Organomet. Chem. 348 (1988) 149;
(c) C. Schunicht, A. Biffis, G. Wulff, Tetrahedron 56 (2000) 1693;
(d) L. Zhu, S.H. Shabbir, M. Gray, V.M. Lynch, S. Sorey, E.V. Anslyn, J. Am. Chem. Soc. 128 (2006) 1222;
(e) Y. Zhang, M. Li, S. Chandrasekaran, X. Gao, X. Fang, H.W. Lee, K. Hardcastle, J. Yang, B. Wang, Tetrahedron 63 (2007) 3287;
(f) T. Aoki, T. Shaki, S. Tsutsui, S. Shinaki, Tetrahedron Lett. 33 (1979) 4569;
(g) A. Ikeda, S. Shinkai, Chem. Rev. 97 (1997) 1713.
[5] E. Hohaus, Z. Anorg. Allg. Chem. 506 (1983) 185.
[6] (a) J.H. Skoog, J. Org. Chem. 29 (1964) 492;
(b) L.K. Mohler, A.W. Czarnik, J. Am. Chem. Soc. 115 (1993) 7037;
(c) N. Farfán, D. Silva, R. Santillan, Heteroatom. Chem. 4 (1993) 533;
(d) J. Trujillo, H. Höpfl, D. Castillo, R. Santillan, N. Farfán, J. Organomet. Chem. 571 (1998) 21.
[7] (a) C.D. Entwistle, T.B. Marder, Chem. Mater. 16 (2004) 4574;
(b) Z. Yuan, J.C. Collins, N.J. Taylor, T.B. Marder, C. Jardin, J.F. Halet, J. Sol. Stat. Chem. 154 (2000) 5;
(c) Z. Yuan, N.J. Taylor, R. Ramachandran, T.B. Marder, Appl. Organomet. Chem. 10 (1996) 305;
(d) W.N. Leng, J. Grunden, G.P. Bartholomew, G.C. Bazan, A.M. Kelley, J. Phys. Chem. (A) 108 (2004) 10050.
[8] C. Lambert, S. Stadler, G. Bourhill, C. Brauchle, Angew. Chem., Int. Ed. Engl. 35 (1996) 644.
[9] I. Cazenobe, I. Ledoux, J. Zyss, A. Thornton, D.W. Bruce, A.K. Kakkar, Chem. Mater. 10 (1998) 1355.
[10] (a) L. Li, G. Li, Y. Wang, F. Liao, J. Lin, Chem. Mater. 17 (2005) 4174;
(b) D. Banerjee, R. Sahoo, R. Debnath, B. Pradhan, T. Kundu, J. Mater. Res. 20 (2005) 1113.

[11] B. del Rey, U. Keller, T. Torres, G. Rojo, F. Agulló-López, S. Novell, C. Martí, S. Brasselet, I. Ledoux, J. Zyss, J. Am. Chem. Soc. 120 (1998) 12808.
[12] H. Reyes, B.M. Muñoz, N. Farfán, R. Santillan, S. Rojas-Lima, P.G. Lacroix, K. Nakatani, J. Mater. Chem. 12 (2002) 2898.
[13] J.L. Maldonado, G. Ramos-Ortíz, O. Barbosa-García, M.A. Meneses-Nava, L. Márquez, M. Olmos-López, H. Reyes, B.M. Muñoz, N. Farfán, Int. J. Mod. Phys. B 21 (2007) 2625.
[14] H. Reyes, Ma. C. García, B.M. Flores, H. López-Rebolledo, R. Santillán, N. Farfán, J. Mex. Chem. Soc. 50 (2006) 106.
[15] M. Rodríguez, Ma.E. Ochoa, R. Santillan, N. Farfan, V. Barba, J. Organomet. Chem. 690 (2005) 2975.
[16] B. Wrackmeyer, Prog. NMR Spectrosc. 12 (1979) 227.
[17] (a) V. Barba, D. Cuautle, R. Santillan, N. Farfán, Can. J. Chem. 79 (2001) 1229;
(b) V. Barba, R. Luna, D. Castillo, R. Santillan, N. Farfán, J. Organomet. Chem. 604 (2000) 273.
[18] H. Höpfl, J. Organomet. Chem. 581 (1999) 129.
[19] (a) H. Höpfl, N. Farfán, J. Organomet. Chem. 547 (1997) 71;
(b) N. Farfán, H. Höpfl, V. Barba, M.E. Ochoa, R. Santillan, E. Gómez, A. Gutiérrez, J. Organomet. Chem. 581 (1999) 70;
(c) V. Barba, G. Vargas, E. Gómez, N. Farfán, Inorg. Chim. Acta 311 (2000) 133.
[20] A. Bondi, J. Phys. Chem. 68 (1964) 441.
[21] (a) H. Zhang, C. Huo, K. Ye, P. Zhang, W. Tian, Y. Wang, Inorg. Chem. 45 (2006) 2788;
(b) G. Rao, Q. Chang, J. Lackowicz, Z. Murtaza, US Pat 6699717B1 (2004);
(c) Z.-L. Wang, Z.-H. Kang, En-Bo Wang, Z.-M. Su, L. Xu, Inorg. Chem. 45 (2006) 4364–4371;
(d) Q. Liu, M.S. Mudadu, H. Schmider, R. Thummel, Y. Tao, S. Wang, Organometallic 21 (2002) 4743.
[22] Y.Q. Li, Y. Liu, W.M. Bu, J.H. Guo, Y. Wang, Chem. Commun. (2000) 1551.
[23] (a) M. Munakata, L.P. Wu, T.K. Sowa, M. Maekawa, Y. Suenaga, G.L. Ning, T. Kojima, J. Am. Chem. Soc. 120 (1998) 8610;
(b) J. Cornil, J-P. Calbert, D. Beljonne, R. Silbey, J.L. Bredas, Adv. Mater. 12 (2000) 978.
[24] (a) J.L. Oudar, J. Chemla, J. Chem. Phys. 66 (1977) 2664;
(b) J.L. Oudar, J. Chem. Phys. 67 (1977) 446.
[25] F. Kajzar, J. Messier, C. Rosilio, J. Appl. Phys. 60 (1986) 3040.
[26] G.M. Sheldrick, SHELX97, Programs for Crystal Structure Solution and Refinement, University of Göttingen, Göttingen, 1997.
[27] L.J. Farrugia, J. Appl. Crystallogr. 32 (1999) 837.
[28] ORTEP 3 L.J. Farrugia, J. Appl. Crystallogr. 30 (1997) 837.
[29] (a) B.F. Levine, C.G. Betha, J. Chem. Phys. 63 (1975) 2666;
(b) B.F. Levine, C.G. Betha, J. Chem. Phys. 65 (1976) 1989.
[30] I. Maltey, J.A. Delaire, K. Nakatani, P. Wang, X. Shi, S. Wu, Adv. Mater. Opt. Electron. 6 (1996) 233.
[31] (a) M.C. Zerner, G. Loew, R. Kirchner, U. Mueller-Westerhoff, J. Am. Chem. Soc. 102 (1980) 589;
(b) W.P. Anderson, D. Edwards, M.C. Zerner, Inorg. Chem. 25 (1986) 2728.
[32] ZINDO, Release 96.0, Molecular Simulations Inc., Cambridge, UK, 1996.
[33] (a) G. Ramos-Ortiz, J.L. Maldonado, M.A. Meneses-Nava, O. Barbosa-García, M. Olmos-López, M. Cha, Opt. Mater. 29 (2007) 636;
(b) G. Ramos-Ortiz, S. Romero, J.L. Maldonado, O. Barbosa-García, M.A. Meneses-Nava, M. Romero, N. Farfán, Rev. Mex. Fís. 52 (2006) 527.
[34] X.H. Wang, D.P. West, N.B. McKeown, T.A. King, J. Opt. Soc. Am. B 15 (1998) 1895.